Colloid Polym Sci 276:289–296 (1998)

ORIGINAL CONTRIBUTION

A. Wurm
M. Merzlyakov
C. Schick

Reversible melting probed by temperature modulated dynamic mechanical and calorimetric measurements

Received: 1 August 1997
Accepted: 24 November 1997

A. Wurm · M. Merzlyakov* · C. Schick (✉)
University of Rostock
Department of Physics
Universitätsplatz 3
D-18051 Rostock
Germany

*On leave from General Physical Institute, Moscow, Russia

Abstract Temperature-modulated DSC (TMDSC) and dynamic-mechanical analysis (DMA) allows the study of degree of crystallinity changes of polymers. From the comparison of the two methods using the same temperature–time program, one expects additional information about the processes occurring in the melting region. A first description of temperature-modulated DMA is given. The effect of reversible melting during every period of temperature modulation has been observed in the melting region of PEEK. The number of molecules which undergo reversible melting for a given quasi-isotherm decreases with time. At 600 K the fraction of the material involved in this process during one modulation cycle is between 0.35% and 0.25%, but has a non-zero value at infinity. The kinetics of this decrease indicates that the process of the structural changes is most likely related to the melt. It can be explained considering an entanglement of the disentangled melt surrounding the just molten crystals. The results are in agreement with the four-state scheme for polymer crystallization and melting proposed by Strobl.

Key words Semicrystalline polymer – PEEK – TMDSC – DMA – melting – crystallization

Introduction

Melting of polymers happens over a broad temperature range (Fig. 1, curve a).

To estimate the latent heat from a common differential scanning calorimetry (DSC) run, one should know the base-line heat capacity contribution to the total heat flow [1, 2]. Considering temperature-modulated DSC (TMDSC), one can expect that the modulated part of the heat flow is that due to base-line heat capacity only. But a TMDSC scan is a quite complicated process since it contains, in addition to the modulation, an underlying heating rate and therefore may show some latent heat effect in each period, influencing the measured heat capacity. Easier to understand are quasi-isothermal measurements with a periodic change of the temperature about a mean temperature. In the case of quasi-isothermal measurements at successive mean temperatures, the influence of the latent heat becomes apparent only at the beginning of each step when the system is brought to a new mean temperature, still, it often takes a long time for the system to reach steady state. As shown by Wunderlich et al. this process is related to reversible melting [3]. In TMDSC experiments such behavior can be observed not only in polymers, but also in low molecular weight liquid crystal compounds [4], see Fig. 2, even at quite small temperature modulation amplitude.

In this paper we are mainly focusing on quasi-isothermal measurements in the melting region of a poly(ether-etherketone) PEEK. Since the changes in degree of crystallinity caused by temperature modulation during one-quasi-isothermal step are less than 11% (see below) it seems to be difficult to examine such small changes in

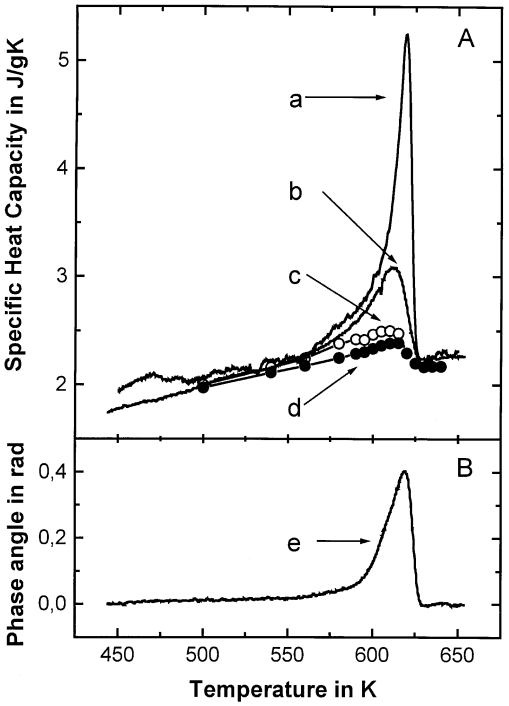

Fig. 1 Heat capacity of PEEK. Part A: calculated from the ratio of heat flow to heating rate for a conventional DSC scan (q_0 = 1 K/min), curve a, and from heat flow amplitude to modulated heating-rate amplitude for temperature-modulated DSC, curve b, and quasi-isothermal measurements, curve c (after 100 s) and curve d (after 1 h). Part B: Phase angle between heating rate and heat flow corrected according to ref. [9] for a temperature modulated scan, curve e. For scan and quasi-isotherm $A_T = 0.2$ K, $t_p = 50$ s

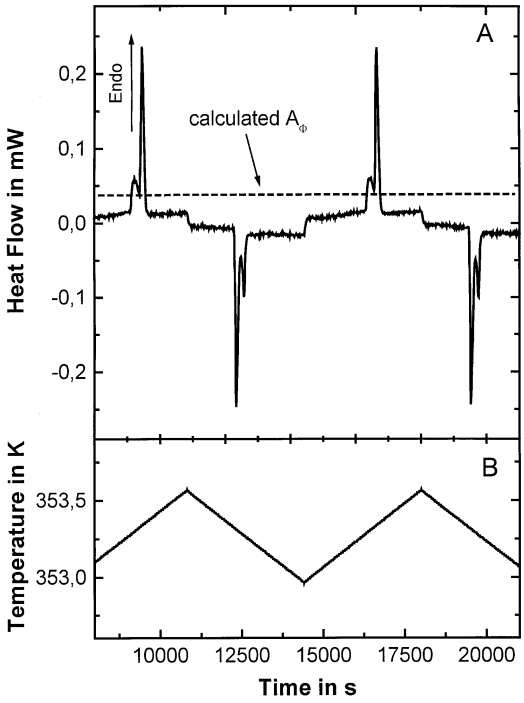

Fig. 2 Measured heat flow for the nematic-isotropic phase transition (during heating) and isotropic-nematic phase transition (during cooling) of 8OCB (curve a) using a quasi-isothermal saw-tooth temperature modulation (curve b) [4]

morphology by X-ray diffraction. On the other hand dynamic mechanical analysis, DMA, is a very sensitive technique to investigate the processes in the melting region. Time-dependent behavior of the heat flow will be compared to the mechanical shear modulus at the same temperature–time program to combine information about the kinetics of melting and crystallization.

Experimental

The PEEK samples were Victrex 381G, supplied by ICI. They were prepared as films with a thickness of 0.05 and 1 mm for DSC and DMA measurements, respectively. For the dynamic-mechanical spectroscopy an ARES spectrometer from Rheometric Scientific has been used. Samples of 6 mm diameter and 1 mm thickness were placed between parallel plates. The resultant torque (τ) by the sample in response to a shear strain (γ) has been measured. First, the linear viscoelastic range was identified by measuring the complex shear modulus as a function of the strain amplitude. The temperature was controlled in an oven with pressurized air by two heaters. The temperature was calibrated using water, indium, tin and lead. A small solid sample of the calibrant was placed between two parallel plates and the change of the length during melting caused by a small compression was measured.

The mechanical storage modulus decreases during melting by more than three orders of magnitude (see inset A in Fig. 3, below). Therefore, it is necessary to vary the shear strain amplitude between 0.1% and 10% to resolve the resultant torque in the measuring range of the mechanical spectrometer. This variation is possible during the measurement with the auto-strain-option which allows to correct the strain amplitude automatically according to the actually measured torque.

TMDSC measurements of the melting behavior of PEEK have been performed with the Perkin-Elmer DSC2 and DSC7 and the Setaram DSC141. Temperature calibration was done according to the GEFTA recommendation [5] and has been checked in the temperature-modulated mode by the smectic-to-nematic transition of 8OCB [4]. In the DSC7 and DSC141 measurement, temperature modulation has been realized by a series of linear heating and cooling cycles (saw-tooth modulation). With the DSC2, a sinusoidal oscillation from an EG&G lock-in

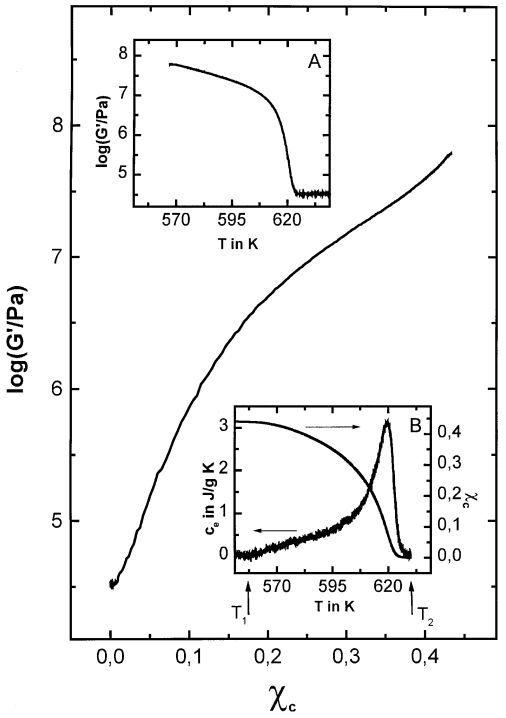

Fig. 3 Relationship between degree of crystallinity, χ_c, and logarithm of storage modulus, G'. Inset A displays the temperature dependence of G'. Inset B shows the excess heat capacity, C_e, vs. temperature $C_e(T) = (\Phi_{dc}(T))/q_0 - C_s(T)$, and the calculated degree of crystallinity, χ_c: $\chi_c(T) = (\int_{T_1}^{T_2} C_e(T')dT' - \int_{T_1}^{T} C_e(T')dT')/\Delta H_{0m} \cdot 100\%$, where T_1 and T_2 are temperatures below and above melting region, respectively. As an approximation $C_s(T)$ is extrapolated as a straight line between $(\Phi_{dc}(T_1))/q_0$ and $(\Phi_{dc}(T_2))/q_0$

amplifier 7220 has been added to the DSC2 temperature-control unit to perform temperature modulation. In case of sinusoidal modulation with the angular frequency $\omega = 2\pi/t_p$ (t_p is the period length) and the amplitude A_T, the temperature of the heater–thermometer block, $T_h(t)$, is given by the equation

$$T_h(t) = T_0 + q_0 t + A_T \sin(\omega t) , \quad (1)$$

where T_0 is the temperature of the starting isotherm, q_0 is a constant, underlying scanning rate. Scanning experiments have been performed only on heating at $q_0 =$ 1 K/min for the DSC2 and DSC7 and at $q_0 = 0.1$ K/min for the DSC141. In quasi-isothermal experiments ($q_0 = 0$) the sample was heated up to the next mean temperature $T_0 + \Delta T$ with $q = 0.1$ K/min after each quasi-isothermal measurement at a given mean temperature T_0. Modulation amplitude A_T and period t_p were the same for quasi-isothermal and scanning measurements namely 0.2 K, 50 s for DSC7, and 0.25 K, 50 s for DSC2, respectively.

For the mechanical measurements the period of the temperature modulation had to be above 600 s because of the long time constant of the equipment. To be able to compare the results, it was necessary to extend the period of TMDSC measurements to the same as used in the temperature-modulated mechanical spectroscopic measurements. But it is difficult to realize temperature modulation with a very long period ($t_p = 1200$ s) and a small amplitude ($A_T = 0.5$ K) with the DSC2 or DSC7 because of the small signal-to-noise ratio under such conditions. To increase the signal-to-noise ratio one has to increase the sample mass. Such higher mass can be used in the Setaram DSC141, but not in the Perkin–Elmer DSC2 or DSC7.

Data-treatment algorithm

A more detailed description of the data treatment for the TMDSC measurements is given in [6–8], it can be summarized as follows:

Consider a system to which some heat flow $\Phi(t)$ is applied to realize some heating rate $q(t)$. The relationship between these functions is

$$\Phi = \tilde{C} q , \quad (2)$$

where $\tilde{C}$ is an operator which transforms the set of functions $\Phi(t)$ to the set of functions $q(t)$. If $\tilde{C}$ is linear, then one can rewrite Eq. (2) as convolution product in time space

$$\Phi = C * q , \quad (3)$$

where $C^* = \tilde{C}$. Applying next the Fourier transform, $F[f](\omega) = (f(t), e^{i(\omega,t)})$, one can rewrite Eq. (3) as

$$F[\Phi] = F[C * q] = F[C]F[q] , \quad (4)$$

where $F[C]$ is a function of angular frequency ω, which can be calculated as

$$F[C](\omega) = \frac{F[\Phi](\omega)}{F[q](\omega)} . \quad (5)$$

When a temperature modulation, as given by Eq. (1), is applied to the system, one can consider total initial heat flow $\Phi(t)$ as the superposition of the underlying heat flow $\Phi_{dc}(t)$ and the periodic heat flow $\Phi_p(t)$

$$\Phi_{dc}(t) = \frac{1}{t_p} \int_{t-t_p/2}^{t+t_p/2} \Phi(t')\,dt' , \quad (6)$$

$$\Phi_p(t) = \Phi(t) - \Phi_{dc}(t) . \quad (7)$$

The phase angle δ is introduced as the phase difference between the periodic heating rate, $q_p(t) = (dT_h/dt) - q_0 = A_T\omega\cos(\omega t) = A_q\cos(\omega t)$, and the first harmonic of

the periodic heat flow, $\Phi_1(t)$ (with a linear response, $\Phi_p(t)$ should be equal to $\Phi_1(t)$)

$$\Phi_1(t) = a\cos(\omega t) + b\sin(\omega t) = \sqrt{a^2 + b^2}\cos(\omega t - \delta)$$
$$= A_\Phi \cos(\omega t - \delta)\,, \tag{8}$$

$$a(t) = \frac{2}{t_p}\int_{t-t_p/2}^{t+t_p/2} \Phi_p(t')\cos(\omega t')\,dt'\,, \tag{9}$$

$$b(t) = \frac{2}{t_p}\int_{t-t_p/2}^{t+t_p/2} \Phi_p(t')\sin(\omega t')\,dt'\,, \tag{10}$$

$$\delta = \arctan(b/a)\,, \tag{11}$$

where A_q is the heating-rate amplitude and A_Φ the amplitude of the first harmonic of the periodic heat flow, respectively. In the general case, factors $a(t)$ and $b(t)$ are time dependent. If $|da(t)/dt| \ll |a(t)|\omega$ and $|db(t)/dt| \ll |b(t)|\omega$, there are negligible changes in heat capacities and thermal conductance over one modulation period. Further, the modulus of the complex heat capacity $|C_\omega|$, is given according to Eq. (5) by the ratio

$$|C_\omega| = \frac{A_\Phi}{A_q}\,. \tag{12}$$

The real part, C'_ω and the imaginary part, C''_ω, of the complex heat capacity are calculated as

$$C'_\omega = |C_\omega|\cos\delta\,, \tag{13}$$

$$C''_\omega = |C_\omega|\sin\delta\,. \tag{14}$$

Temperature modulation can also be applied to DMA measurements. As shown in Fig. 7 curve b, below, the storage modulus follows the programming temperature in such a way that during heating there is always a decrease and during cooling an increase. Thus, the same data treatment as for the heat capacity can be used for the storage modulus, $G'(t)$. The term $A_{G'}$ is introduced for the mechanical storage modulus amplitude. Since the mechanical modulus decreases by three orders of magnitudes during melting, (see Fig. 3), it is better to normalize $A_{G'}$ for comparison at different temperatures. For this normalization, $A_{G'}$ is divided by the absolute value of the storage modulus G' to get a fractional amplitude that represents the relative changes in shear modulus due to temperature modulation. In the same way as in TMDSC, a phase angle between storage modulus and temperature profile can be introduced. But the results obtained are not representative because of the low signal-to-noise ratio.

Next, we come back to the TMDSC measurements and discuss some problems that can arise in interpretation of complex heat capacities.

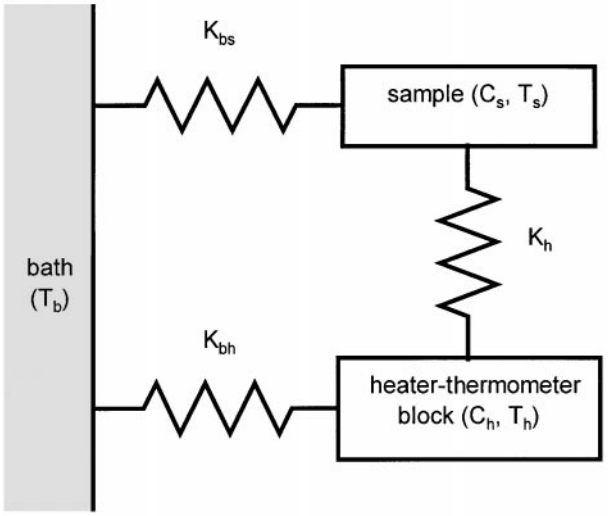

Fig. 4 Diagram of a sample connected to a bath and heater-thermometer block by thermal conductances K_{bs} and K_h, respectively

The problem of phase angle

One problem of the phase angle is connected with the DSC technique where the measured temperature is the temperature of the heater-thermometer block, rather than the sample temperature. Consider a system, as in Fig. 4, consisting of a heater–thermometer block and sample, each is assumed to have infinite thermal conductivity and heat capacities C_h and C_s, respectively. These components are interconnected by thermal conductances K_h, K_{bh}, K_{bs}, as indicated in Fig. 4. If the temperature variations are sufficiently small and there is no thermal process inside the sample, the various heat capacities and thermal conductivities may be considered constant. Further, in case of a well-balanced DSC, the small values of K_{bh}, K_{bs} and C_h can be neglected. The heat-flow equation for the system is then

$$\Phi(t) \equiv C_s\frac{dT_s(t)}{dt} = K_h(T_h(t) - T_s(t))\,. \tag{15}$$

Next, we consider a case with quasi-isothermal sinusoidal temperature modulation applied to the system (as in Eq. (1) with $q_0 = 0$). The phase angle due to finite thermal conductance between sample and heater–thermometer block, ε, is given by

$$\varepsilon = \arctan\left(\frac{\omega C_s}{K_h}\right). \tag{16}$$

Thus, the measured phase angle, determined by Eq. (11), should be corrected by ε to apply to the complex heat capacity

$$C'_\omega = |C_\omega|\cos(\delta - \varepsilon)\,, \tag{13'}$$

$$C''_\omega = |C_\omega| \sin(\delta - \varepsilon) \,. \tag{14'}$$

The problem for this correction is the exact determination of C_s/K_h. Usually, the value $|C_\omega| = A_\Phi/A_q$ is taken for C_s and K_h and is calculated assuming that $\delta - \varepsilon$ should be zero in temperature regions where no thermal processes occur inside the sample [9]. Next, we assume that one has a scanning run with such a small modulation amplitude that the sample is always heated ($A_q < q_0$) and with such long modulation period that melting can be considered as a continuous process. Then the thermal equation is given as

$$\Phi(t) \equiv (C_s + C_e)\frac{dT_s(t)}{dt} = K_h(T_h(t) - T_s(t)) \,, \tag{17}$$

where C_e is the excess heat capacity of the process and

$$C_s + C_e = \frac{\Phi_{dc}}{q_0} > \frac{A_\Phi}{A_q} = |C_\omega|$$

(see curves a and b in Fig. 1). Then

$$\varepsilon = \arctan\left(\frac{\omega(C_s + C_e)}{K_h}\right) > \arctan\left(\frac{\omega|C_\omega|}{K_h}\right).$$

From this follows that it is still an open question which part of the phase angle in the melting region (Fig. 1, curve e) corresponds to the sample properties. Even if the effect is large, as one may argue, there is also a large contribution to the heat flow from the heat of fusion, that is C_e, and therefore a large part of the phase lag may be caused by heat transfer [10].

The problem of complex heat capacity

Another problem concerning data treatment is the restriction of the Fourier formalism. If one considers an example of reversible melting during every modulation period, as in Fig. 2, A_Φ (dotted line in the figure) is higher than the heat flow due to heat capacity (i.e. the heat flow outside the melting and crystallization regions) because it contains a large contribution from the melting and crystallization peaks (the melting and crystallization enthalpies). One can double the temperature amplitude at a given frequency, i.e. double the heating rate, but would get almost the same response in the first harmonic of the heat-flow amplitude since the melting and crystallization areas do not change. Then, the calculated value of the modulus of the complex heat capacity will be almost half. As for the phase angle, it is mainly determined by the position of the melting and crystallization peaks added to the heat flow profile and it changes drastically with changes of the mean temperature, T_0, even when these changes are lower than the modulation amplitude, T_a [4].

In the above example the system did not show linear response and cannot be described by Eq. (3). In this case it is not allowed to consider only the complex heat capacity determined by Eqs. (12)–(14). Therefore, it is better as a first step to look at the total measured initial heat flow profile to see whether it is reasonable to perform further calculations.

In the present paper we do not interpret the phase angle and the modulus of the complex heat capacity for this reason and discuss only the heat flow as a function of time. Investigating heat flow profiles, it is sometimes better to have a rectangular profile of heating rate, i.e. a saw-tooth temperature modulation. To notice the changes in the meander-shaped heat flow is easier than in the case of sinusoidal temperature modulation (some examples are given in [11, 12]).

Results and discussions

In Part A of Fig. 5 the heat-flow amplitudes are given from scanning and quasi-isothermal TMDSC measurements of PEEK, but with a much longer temperature-modulation period than shown in Fig. 1.

Fig. 5 A: Modulated heat-flow amplitudes from TMDSC scan (curve a) and quasi-isothermal TMDSC measurements, curve b (after 0.5 h) and curve c (after 3 h). B: Normalized amplitude of the mechanical storage modulus from temperature-modulated dynamic mechanical spectroscopy. $A_T = 0.5$ K, $t_p = 1200$ s

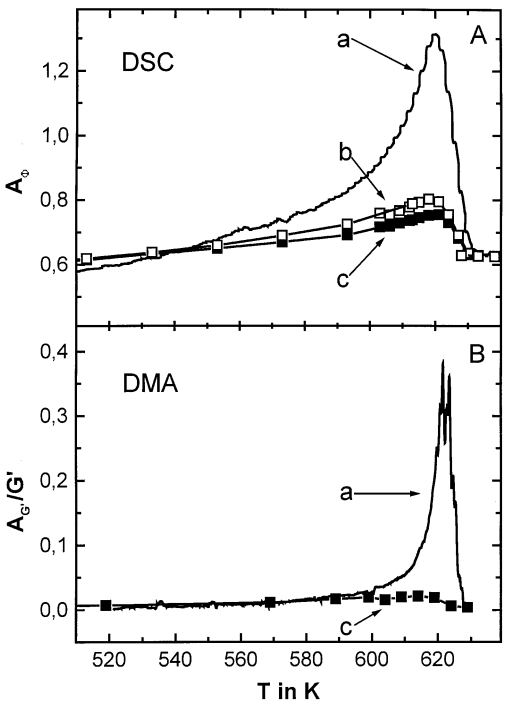

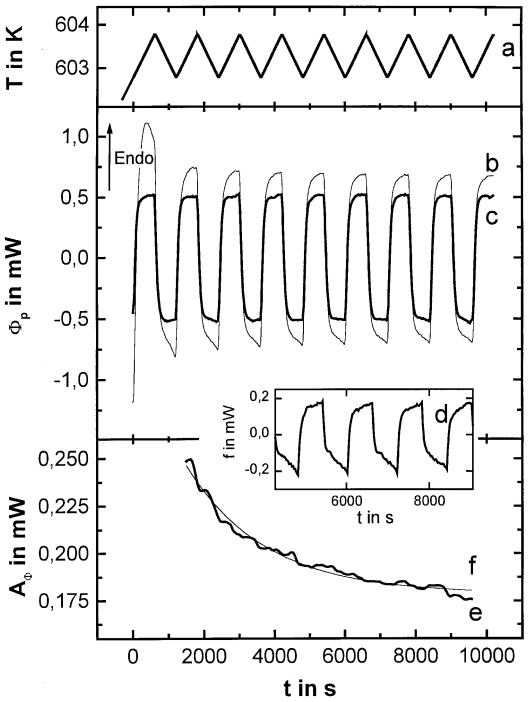

Fig. 6 Temperature-modulated DSC. Curve a: Saw-tooth temperature modulation. Curve b: modulated part of the heat flow at 603 K. Curve c: the same from the melt at 640 K. Curve d: difference between curves b and c. Curve e: amplitude of the difference between curves b and c. Curve f: exponential fit, $f = A + B \exp\{-t/\tau_a\}$

In the mechanical measurements with the same temperature-time program (part B) one can detect a peak in the curve of the normalized amplitude of the mechanical storage modulus from temperature-modulated scans and quasi-isotherms.

Figure 6 shows, next, the periodic heat flow, $\Phi_p(t)$, for one quasi-isothermal TMDSC measurement, where curve b is the periodic heat flow in the melting region and curve c is the periodic heat flow in the melt. Even after a long time, the heat-flow amplitude in the melting region is still bigger than that in the melt. One must, thus, conclude that in addition to the base-line heat capacity there is a continuing contribution due to melting and crystallization. One can assume that the heat capacity, C_s, of the semicrystalline material in the melting region is close to that of the totally melted material. Then the difference, given by curve d on Fig. 6 is

$$f(t) = \Phi_p(t)|_{\text{in melting region}} - \Phi_p(t)|_{\text{in the melt}} , \tag{18}$$

where $f(t)$ represents the reversible melting (positive part) and crystallization (negative part).

From the shape of curve d (Fig. 6) one can see that melting and crystallization processes influence the heat flow profile differently, so that during heating the system comes to steady state faster than during cooling. Such observations would be impossible by calculating heat flow amplitude and phase angle only. From $f(t)$ one can calculate the reversible changes of enthalpy, Δh, during one period

$$\Delta h = \int_{t_1}^{t_2} f(t)\,\mathrm{d}t \approx \frac{A_f t_p}{\pi} , \tag{19}$$

where t_1 and t_2 are points within one period at which $f(t_1) = f(t_2) = 0$, and A_f is the amplitude of $f(t)$, calculated the same way as A_Φ for $\Phi_p(t)$. As shown in the figure by curve f, A_f decreases with time to some nonzero value. Knowing the enthalpy of fusion of the fully crystallized PEEK ($\Delta H_{0m} = 130$ J/g), one can also estimate the reversible change of crystallinity $\Delta\chi_c$ during one period

$$\Delta\chi_c = \frac{\Delta h}{\Delta H_{0m}} \cdot 100\% .$$

At 600 K, for instance, this change equals 0.35% at the beginning of the experiment and 0.25% at the end.

The underlying heat-flow rate, Φ_{dc}, changes greatly at the beginning of the quasi-isotherm because of new melting on changing from the lower temperatures (which influences $\Phi_p(t)$ at the first half period, Fig. 6). This is followed by some additional changes during the quasi-isotherm. Knowing these changes in Φ_{dc} allows to estimate the overall change in crystallinity during one quasi-isotherm, but the changes in underlying heat flow are close to detection limit of the equipment (0.05 mW for DSC141) which is determined by the total heat-flow drift during the long measuring time. As shown below, the overall changes in crystallinity are easier to determine with the DMA measurements.

The degree of crystallinity calculated by standard DSC (see Fig. 3) can be compared to the mechanical storage modulus. In the temperature region of 580–610 K, the degree of crystallinity has a close linear relationship to the logarithm of the mechanical storage modulus. This allows estimation of changes in crystallinity from changes in mechanical storage modulus as shown in Fig. 3.

Figure 7 shows the temperature–time program and the behavior of the mechanical storage modulus for one quasi-isotherm. The mechanical storage modulus (during the heating step) decreases (i.e. melting process) and during cooling it always increases (i.e. crystallization). At 599 K, the sample has a degree of crystallinity, χ_c, close to 30% (see Fig. 3, inset B). An estimate of the reversible changes of crystallinity during one period can be obtained from the amplitude of the mechanical storage modulus $A_{G'}$. It gives a value of 0.3%, or about 1% of the crystalline fraction – the same as obtained from TMDSC. Unfortunately, because of the low signal-to-noise ratio, it is impossible to

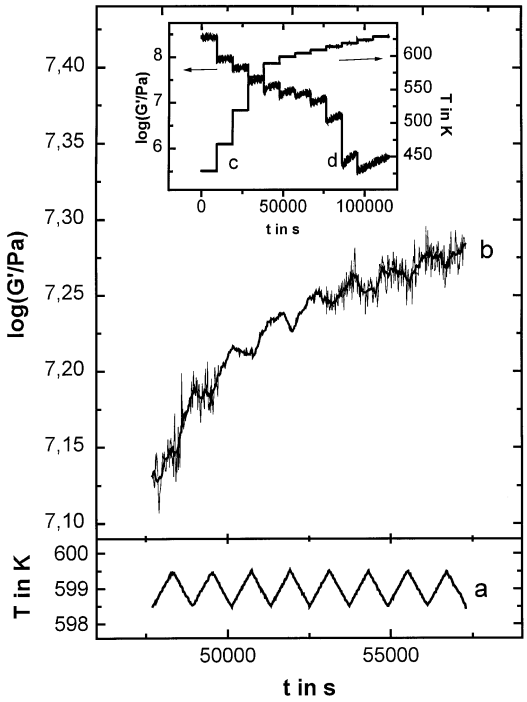

Fig. 7 Temperature-modulated DMA. Curve a: temperature modulation profile. Curve b: logarithm of the mechanical storage modulus G' of the quasi-isotherm at 599 K. Between 50 000 s and 52 500 s only the average line is shown. The Inset shows the whole time–temperature program (curve c) and the behavior of the mechanical storage modulus for the quasi-isothermal measurements at different temperatures (curve d)

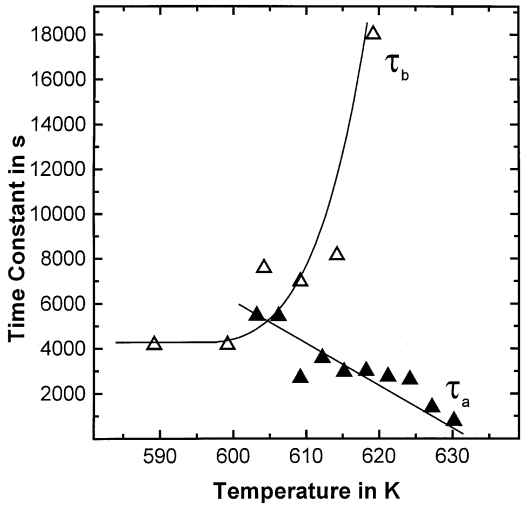

Fig. 8 Time constants for reversible, τ_a, and for overall, τ_b, change of crystallinity at different quasi-isothermal temperatures. The lines are guides for the eye

follow the dynamics of the change of $A_{G'}$ with time as can be done for A_f in TMDSC. But the underlying increase of the mechanical storage modulus G' with time is quite remarkable (Fig. 7) and not detectable in TMDSC. Thus, both TMDMA and TMDSC methods supplement each other. The same way as for reversible part, one can estimate overall increase of crystallinity during one quasi-isotherm from the change of mechanical modulus. For example at 599 K this increase is about 3%.

From these results of reversible and overall changes in crystallinity, one can conclude that at any point within the melting range of PEEK a certain fraction of the macromolecules can undergo reversible melting. Over longer time periods, increasing numbers of these molten molecules are removed from the reversible process (analogous result has been obtained in Ref. [3] for PET). But it is unclear whether they melt completely or rearrange to a more perfect crystalline domain. To better understand in which direction this process goes, one can compare dynamics of reversible and overall changes in crystallinity. For these purposes one may fit the time-dependent A_f with an exponential decay function and introduce a time constant τ_a to estimate the kinetics of changes in the reversible process (curve *f* in Fig. 6). It is a question of the model used which type of function is suitable for the fit, for example, a second-order exponential decay function as was used in [3]. But one-time constant may be enough for a rough estimate. The same way another time constant τ_b is introduced for the overall increase of crystallinity by applying an exponential fit to the logarithm of the mechanical storage modulus (curve b in Fig. 7).

From Fig. 8 it is clear that the overall increase of crystallinity and the reversible melting are independent processes. The rate of overall increase of crystallinity becomes smaller with increasing temperature, in contrast, the reversible melting comes to equilibrium increasingly faster. This indicates that reversible melting is a local process, independent of the background of overall crystallization.

Conclusions

The effect of reversible melting during every period of temperature modulation has been observed in the melting region of PEEK. A method to estimate the change in crystallinity due to this reversible process using DMA and TMDSC has been demonstrated. Parallel results have been obtained by both techniques. The amount of crystallinity involved in reversible melting for a given quasi-isotherm decreases with time (crystallinity involved in this process at 600 K is between 0.35% and 0.25%), but does not becomes zero at infinite time. Its time dependence can be simply fitted by an exponential decay function. The

higher the temperature, the faster the relaxation of the reversible melting. This indicates that the relaxation process is most likely related to the melt. Our findings support the idea of Strobl [13, 14] that melting of a polymer crystal takes place at an equilibrium between the crystal and a partially disentangled melt. The decrease of the amplitude of the reversible melting may be related to the change of the partially disentangled melt to the entangled equilibrium state of the melt which does not allow crystallization without super-cooling. On the other hand, the process of increasing overall crystallization during quasi-isotherm becomes slower with increasing temperature.

Another interesting observation is that the time–temperature behavior of the heat-flow amplitude in quasi-isothermal measurements (i.e. relaxation from beginning to end) is qualitatively the same for short and long periods (compare Fig. 1 and Fig. 5) but with different time scales. For example at 600 K $\tau_a = 770$ s for $t_p = 50$ s and $\tau_a = 5500$ s for $t_p = 1200$ s. Thus, the relaxation process has some frequency dependence. The one possible explanation of this is that with longer modulation, period longer-time-consuming processes are involved in this reversible melting. On the other hand, the amplitude of reversible melting should depend on the temperature–modulation amplitude. All these questions need further investigations.

Acknowledgements This work was financially supported by the European Commission and the government of Mecklenburg-Vorpommern. The authors would like to thank B. Wunderlich (Oak Ridge National Laboratory) and J.E.K. Schawe (University of Ulm) for helpful discussions.

References

1. Mathot VBF (1994) Calorimetry and Thermal Analysis of Polymers. Carl Hanser Verlag
2. Alsleben M, Schick C (1994) Thermochim Acta 238:203
3. Okazaki I, Wunderlich B (1997) Macromol Chem Rapid Commun 18:313
4. Hensel A, Schick C (1997) Thermochim Acta 304/305:229
5. Sarge SM, Hemminger W, Gmelin E, Höhne GWH, Cammenga H, Eysel W (1997) J Thermal Anal 49:1125
6. Schawe JEK (1995) Thermochim Acta 260
7. Reading M (1993) Trends Polym Sci 8:248
8. Wunderlich B, Jin Y, Boller A (1994) Thermochim Acta 238:277–293
9. Weyer S, Hensel A, Schick C (1997) Thermochim Acta 304/305:267
10. Merzlyakov M, Schick C (in preparation)
11. Ishikiriyama K, Wunderlich B (1997) Macromolecules 30:4126
12. Ishikiriyama K, Wunderlich B (1997) J Polymer Sci, Part B. Polymer Phys 35:1877
13. Strobl G (1997) Acta Polymerica 48:562
14. Schmidtke J, Strobl G, Thurn-Albrecht T (1997) Macromolecules 30:5804